

# Can Amphipathic Helices Influence the CNS Antinociceptive Activity of Glycopeptides Related to $\beta$ -Endorphin?

Yingxue Li,<sup>†</sup> Lindsay St. Louis,<sup>‡</sup> Brian I. Knapp,<sup>§</sup> Dhanasekaran Muthu,<sup>†</sup> Bobbi Anglin,<sup>†</sup> Denise Giuvelis,<sup>‡</sup> Jean M. Bidlack,<sup>§</sup> Edward J. Bilsky,<sup>‡</sup> and Robin Polt<sup>\*,†</sup>

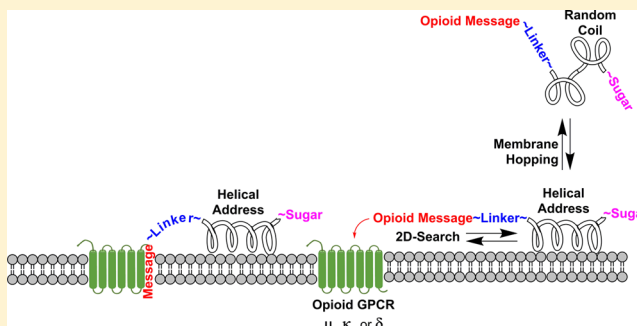
<sup>†</sup>Department of Chemistry & Biochemistry and BIOS, The University of Arizona, Tucson, Arizona 85721, United States

<sup>‡</sup>Department of Biomedical Sciences, COM and Center for Excellence in the Neurosciences, University of New England, Biddeford, Maine 04005, United States

<sup>§</sup>Department of Pharmacology, University of Rochester Medical Center, Rochester, New York 14642, United States

## S Supporting Information

**ABSTRACT:** Glycosylated  $\beta$ -endorphin analogues of various amphipathicity were studied in vitro and in vivo in mice. Opioid binding affinities of the O-linked glycopeptides (mono- or disaccharides) and unglycosylated peptide controls were measured in human receptors expressed in CHO cells. All were pan-agonists, binding to  $\mu$ -,  $\delta$ -, or  $\kappa$ -opioid receptors in the low nanomolar range (2.2–35 nM  $K_i$ 's). The glycoside moiety was required for intravenous (i.v.) but not for intracerebroventricular (i.c.v.) activity. Circular dichroism and NMR indicated the degree of helicity in H<sub>2</sub>O, aqueous trifluoroethanol, or micelles. Glycosylation was essential for activity after i.v. administration. It was possible to manipulate the degree of helicity by the alteration of only two amino acid residues in the helical address region of the  $\beta$ -endorphin analogues without destroying  $\mu$ -,  $\delta$ -, or  $\kappa$ -agonism, but the antinociceptive activity after i.v. administration could not be directly correlated to the degree of helicity in micelles.



## INTRODUCTION

It is estimated that there are 1.5 billion people worldwide suffering at any given time from some type of central nervous system (CNS) disorder. Novel CNS drugs have the potential to further improve quality of life and to reduce the disease burden for these serious diseases and disorders.<sup>1</sup> Since the discovery of the two endogenous pentapeptides, Met-enkephalin and Leu-enkephalin, in 1975, more than 250 endogenous neuropeptides have been identified, and there is now a broad vista for the application of these peptides in pharmacology, especially for the opioids that are so widespread throughout the CNS.<sup>2</sup> Now in the fourth decade of research in this area, many potent and selective peptide agonists have been developed for the three cloned opioid receptors, but some crucial drawbacks still persist that dampen enthusiasm for the use of these compounds as peptide-based drugs, primarily instability in vivo and poor blood–brain barrier (BBB) penetration.

Numerous methods have been devised and successfully applied to overcome metabolic instability and high clearance of peptides.<sup>3</sup> The principal problem remaining is poor penetration of the BBB.<sup>4</sup> The BBB a component of the neurovascular unit, a structure consisting of endothelial cells of brain and spinal cord capillaries, astrocytes, basement membrane, pericytes, and neurons in physical proximity to the endothelium that varies in composition and function from site to site within the brain.<sup>5</sup>

It is known that the BBB has anatomic and neuroprotective functions because of the presence of oxidative enzymes and peptidases such as aminopeptidase, arylamidase, and enkephalinase.<sup>6</sup> Thus, opioid peptides are generally degraded before they penetrate the CNS. The ability of drugs to diffuse passively across the BBB has been predicted by molecular size, charge, hydrogen bonding, and lipid solubility, but it is not clear how applicable Lipinski's rules are to peptides.<sup>3,7,8</sup> Several modifications have been studied in an effort to overcome the BBB penetration problem, including lipidization,<sup>9</sup> structural modification to enhance stability,<sup>10</sup> glycosylation,<sup>11</sup> nutrient transporters,<sup>12</sup> prodrugs,<sup>13</sup> vector-based Trojan horses,<sup>14</sup> cationization,<sup>15</sup> and conjugation to or encapsulation by polymers.<sup>16</sup> Glycosylation has been shown to improve antinociceptive potency and bioavailability of glycopeptides via higher metabolic stability,<sup>17</sup> reduced clearance,<sup>18</sup> and improved BBB transport.<sup>19</sup> Some BBB penetration studies with glycopeptide agonists related to enkephalins have shown up to a 3-fold increase in the rate of brain delivery of these analogues compared with the unglycosylated parent peptides.<sup>20</sup> Recent studies with glycopeptides in micelles indicate that amphipathicity of the glycopeptides is an important factor in

Received: August 9, 2013

Published: February 27, 2014

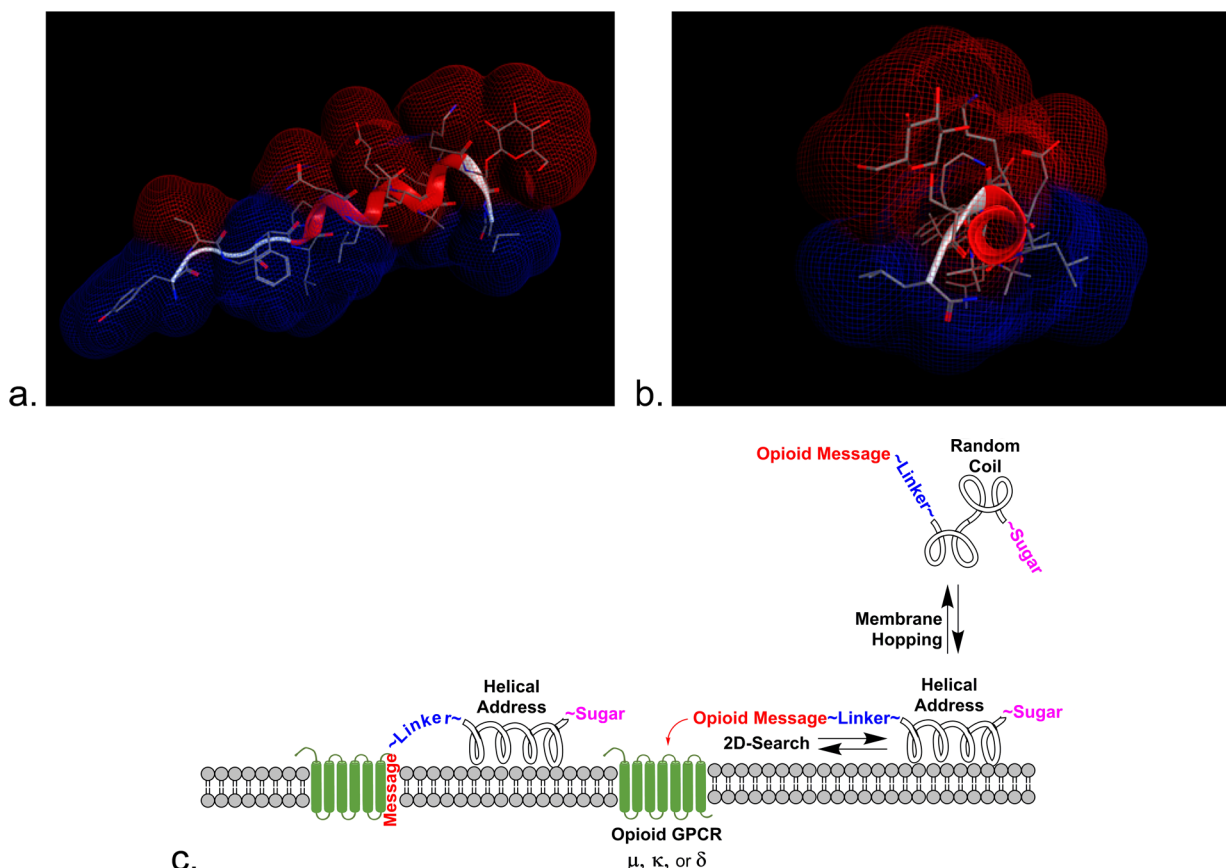


**Figure 1.** Reduction of dimensionality. The calculated hydrophilic (red) and hydrophobic (blue) Connolly surfaces are illustrated for glycopeptide L1 in side view (a) and down the axis of the helical address region (b). The 9th and 12th residues were replaced by  $\alpha$ -aminoisobutyric acid (Aib), alanine, or glycine to adjust the helicity by increments. (c) The sugar can play an important role in drug transport by pulling the glycopeptide away from membranes into the aqueous milieu to enable membrane hopping.<sup>34,35</sup> The amphipathic helix promotes 2D searching of the membrane in order to facilitate receptor binding.<sup>64,65</sup>

BBB penetration.<sup>21</sup> It has been suggested that glycosylation can alter tissue distribution patterns of glycopeptide drugs<sup>22</sup> and affect interactions with receptors.<sup>21a,23</sup>

**Endogenous Neuropeptide Conformations.** The endogenous opioid  $\beta$ -endorphin has the Met-enkephalin peptide sequence YGGFM~ at the N-terminus and consists of 31 residues. It binds preferentially to  $\mu$  and  $\delta$  receptors over  $\kappa$ -opioid receptors.<sup>24,25</sup> Kaiser and co-workers synthesized several  $\beta$ -endorphins with the Met-enkephalin sequence, a hydrophilic linking segment, S- $\gamma$ -amino- $\gamma$ -hydroxymethylbutyric acid (HOME-GABA), replacing residues 6–12, and an amphiphilic helical segment between the helix breaker residues Pro(13) and Gly(30). The circular dichroism (CD) spectra of all mimics, with minimal homology to the  $\beta$ -endorphin sequence, showed minima at 210 and 222 nm, indicative of  $\alpha$ -helical structure.<sup>26</sup> Compared to  $\beta$ -endorphin, the peptide mimics were 2 to 3 times more potent in  $\mu$ - and  $\kappa$ -opioid receptor binding assays, about equipotent in the  $\delta$ -receptor binding assay, and possessed strong resistance toward proteolytic enzymes.<sup>27</sup> These findings strongly suggested that the amphipathic  $\alpha$ -helical structure in the C-terminal region of  $\beta$ -endorphin plays a key role in receptor binding and opioid activity as well as resistance to proteolysis of mimic analogues. Kyle and co-workers designed and synthesized several conformationally constrained nociceptin (NC/ORL-1) analogues,<sup>28</sup> where they exploited the  $\alpha$ -helical-promoting residues  $\alpha$ -aminoisobutyric acid (Aib) and N-methyl alanine (MeAla) as replacement(s) for Ala<sub>7</sub>, Ala<sub>11</sub>, or

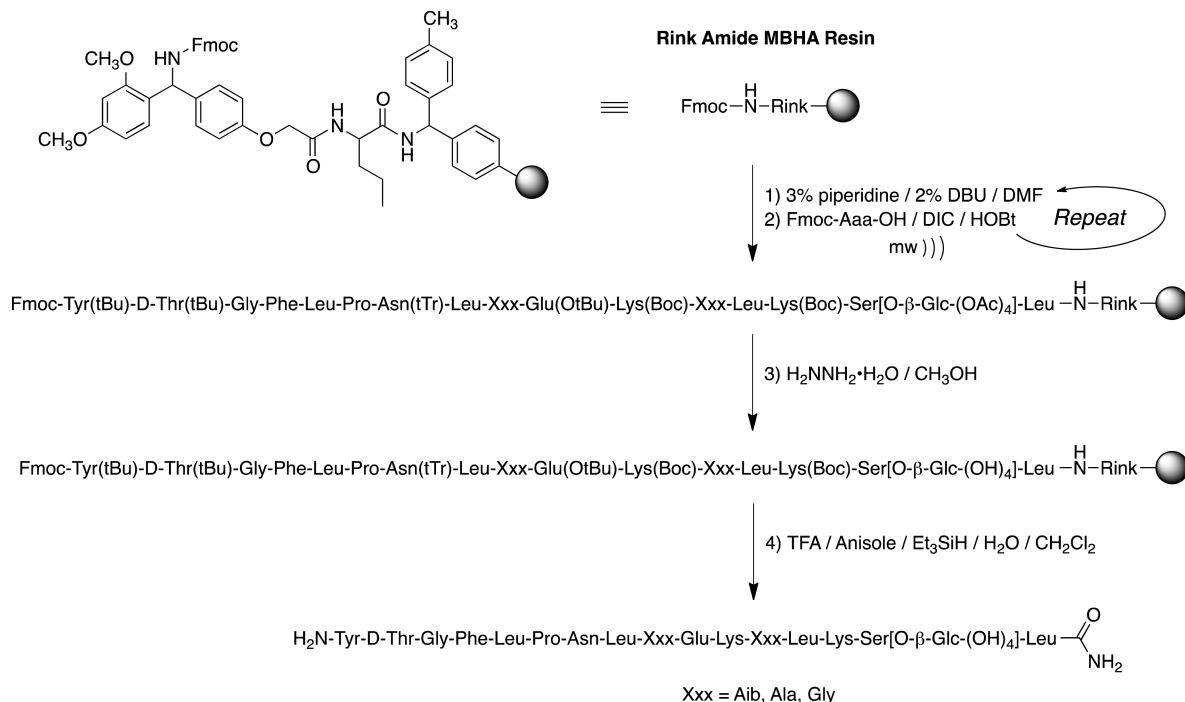
Ala<sub>15</sub> in the native NC C-terminal sequence. The importance of  $\alpha$ -helical address segments of peptides has also been demonstrated in the secretin family of peptide receptors, including CRF, secretin, and VIP. The interaction of PACAP<sub>1–38</sub> with a phospholipid membrane has been shown to be involved in binding and receptor specificity, increasing peptide stability, and amplifying bioactivity in vivo.<sup>29</sup>

**Glycopeptide Design Principles.** On the basis of the evidence that glycosylation decreases lipophilicity and on the hypothesis that amphipathic properties of the helix could help guide a membrane-associated peptide to its specific receptor, three generations of glycosylated  $\beta$ -endorphin analogues have now been synthesized for study:<sup>30</sup> the first bearing longer helices<sup>21a</sup> too stable to engage in bioluminescent behavior,<sup>30</sup> the second being this study,<sup>21b</sup> and the third bearing more flexible linkages between the opioid message and the helix address, which will be published shortly. It is of interest that some of the longer endorphin glycopeptides analogues penetrated the BBB at higher rates than the shorter enkephalin glycopeptide analogues.<sup>21b</sup> The influence of the amphipathic helix in tandem with glycosylation on drug delivery is therefore of great interest and was further examined using a series of  $\beta$ -endorphin glycopeptide analogues of varying helicity and bearing different sugar moieties. To understand the conformation and dynamics of membrane-bound peptides or integral proteins, several model systems have been developed to mimic features of the membrane. It is generally accepted that the detergent sodium

Table 1. Peptide/Glycopeptide Sequences<sup>a</sup>

$S^{\circ} = S$ OH	$S^{\circ} = S^*$ $\beta$ -glucose	$S^{\circ} = S^{**}$ $\beta$ -lactose	helix determinant	message~Pro <sub>6</sub> ~helix-amide
U1	G1	L1	~B~B~	YtGFL-P <sup>6</sup> -NLB <sup>9</sup> EKB <sup>12</sup> LKS <sup>15</sup> L-NH <sub>2</sub>
U2	G2	L2	~A~B~	YtGFL-P <sup>6</sup> -NLA <sup>9</sup> EKB <sup>12</sup> LKS <sup>15</sup> L-NH <sub>2</sub>
U3	G3	L3	~B~A~	YtGFL-P <sup>6</sup> -NLB <sup>9</sup> EKA <sup>12</sup> LKS <sup>15</sup> L-NH <sub>2</sub>
U4	G4	L4	~A~A~	YtGFL-P <sup>6</sup> -NLA <sup>9</sup> EKA <sup>12</sup> LKS <sup>15</sup> L-NH <sub>2</sub>
U5	G5	L5	~A~G~	YtGFL-P <sup>6</sup> -NLA <sup>9</sup> EKG <sup>12</sup> LKS <sup>15</sup> L-NH <sub>2</sub>
U6	G6	L6	~G~A~	YtGFL-P <sup>6</sup> -NLG <sup>9</sup> EKA <sup>12</sup> LKS <sup>15</sup> L-NH <sub>2</sub>
U7	G7	L7	~G~G~	YtGFL-P <sup>6</sup> -NLG <sup>9</sup> EKG <sup>12</sup> LKS <sup>15</sup> L-NH <sub>2</sub>

<sup>a</sup>S = L-serine, S\* =  $\beta$ -O-glucosyl-L-serine, S\*\* =  $\beta$ -O-lactosyl-L-serine, and B =  $\alpha$ -aminoisobutyric acid (Aib).

Scheme 1. Glycopeptide Synthesis<sup>a</sup>

<sup>a</sup>Fmoc construction of the glycopeptides using DIC/HOBt coupling with microwave heating was applied to MBHA-functionalized Rink polystyrene resin. Fmoc deprotection was accomplished with 3% piperidine/2% DBU in DMF. Treatment with H<sub>2</sub>NNH<sub>2</sub>·H<sub>2</sub>O was required to remove the acetates from the glycoside moiety prior to cleavage from the Rink resin using TFA/PhOCH<sub>3</sub>/Et<sub>3</sub>Si/H<sub>2</sub>O in CH<sub>2</sub>Cl<sub>2</sub> to provide the C-terminal amides.

dodecyl sulfate (SDS) mimics the membrane-like environment and therefore its use has been reported in the literature extensively to study peptide–membrane interactions.<sup>21b,31</sup> Schwyzer's membrane compartment concept<sup>23</sup> suggests that amphipathic helices<sup>32</sup> will promote binding with the receptors via a 2D search of the membrane rather than a 3D search of the aqueous compartment (cf. reduction of dimensionality; Figure 1).<sup>33</sup>

According to detailed analysis of globular proteins physical-chemical and structural properties, Segrest and co-workers grouped amphipathic helices into different classes (A, H, L, G, K, C, and M)<sup>34</sup> according to the geometric distribution of lipophilic and hydrophilic residues. Class H, polypeptide hormones, typically contain two distinct functional domains, a short N-terminal domain including a specific *message* segment that binds to the transmembrane portion of the receptor and a much longer amphipathic helix, or *address* segment, located at the C-terminal portion of the peptide. The helical domain may provide enhanced receptor targeting in a relatively nonspecific manner by increasing affinity for the hydrophobic membrane

that contains the receptor. It has been proposed that peptide–lipid interaction leading to cell penetration plays a major role in their activity by one of two general mechanisms: (1) transmembrane pore formation via a barrel-stave mechanism and (2) membrane destruction/solubilization via a carpet mechanism.<sup>35</sup> It is proposed that exploitation of the first step of these mechanisms by class H glycopeptides will allow for reversible adsorption to biological membranes without membrane disruption. This putative glycopeptide–lipid interaction allows peptides with amphipathic helix conformation to float in the cell membrane, exposing the hydrophobic side to the hydrophobic membrane and the hydrophilic side to the aqueous exterior of the cell. Furthermore, it is proposed that this transient interaction with biological membranes is essential for crossing cellular barriers (not membranes), such as the endothelial layer of cells that compose an important part of the BBB.

The peptides and glycopeptides examined in the current studies were designed in accordance with Kaiser's classic studies of  $\beta$ -endorphin<sup>24–27</sup> combined with a simple Edmundson



wheel approach to introduce amphipathicity per Segrest's insights.<sup>36</sup> Molecular mechanics calculations confirmed the potential for helical amphipathic structures for the glycopeptides. In this study, all of the glycopeptides shared the same message segment, YtGFL~, used in previously published studies.<sup>21</sup> The helix-breaking residue Pro<sup>6</sup> was used to link the N-terminal message domain and C-terminal helix. The three series (Table 1) bore either an unglycosylated L-serine residue (U series), an L-serine monosaccharide bearing a  $\beta$ -O-glucose (G series), or an L-serine disaccharide bearing a  $\beta$ -O-lactose (L series). Each series of seven ligands differed in the address domain sequence residues at position 9 or 12, where Aib, Ala, and Gly were introduced into the C-terminal address to obtain different helix propensities.<sup>21b,36</sup> All of the helical conformations were presumably stabilized by a salt bridge between Glu<sub>10</sub> and Lys<sub>14</sub> ( $i \rightarrow i + 4$ ).<sup>37</sup>

## EXPERIMENTAL DETAILS

**Materials.** The Fmoc-protected amino acids and the Rink amide MBHA resin (4-(2',4'-dimethoxyphenyl-fmoc-aminomethyl)-phenoxy-acetamido MBHA, grain size: 100–200 mesh, substitution 0.83 mmol/g) were obtained from Chem-Impex International. Sodium dodecyl-*d*<sub>25</sub> used in NMR experiments was purchased from CDN Isotopes Inc., Canada. All other reagents and solvents were purchased from Aldrich Co. and used without further purification.

**Peptide Synthesis and Purification.** The Fmoc-protected serine glycosides were prepared using published procedures.<sup>38–41</sup> The glycopeptides were synthesized manually using established solid-phase Fmoc-chemistry methodology with Rink amide MBHA resin (substitution: 0.83 meq/g, 1% DVB).<sup>42,43</sup> The side-chain-protected amino acids used in the synthesis were Fmoc-Lys(Boc)-OH, Fmoc-Glu(OtBu)-OH, Fmoc-Asn(Trt)-OH, Fmoc-D-Thr(But)-OH, and Fmoc-Tyr(But)-OH. Coupling of all the Fmoc-protected amino acids was performed in a sealed tube heated by an Emerson 900 W microwave oven at power level 1 for 10 consecutive minutes. Coupling was performed (2.0 equiv Fmoc-AA compared to resin) using 1-hydroxybenzotriazole (HOBt, 2.0 equiv) and *N,N'*-diisopropylcarbodiimide (DIC, 2.0 equiv) in a 1:1 mixture of dimethylformamide (DMF) and *N*-methylpyrrolidone (NMP) (Scheme 1). Coupling was monitored using Kaiser's ninhydrin test. The Fmoc groups were removed using a mixture of 3% piperidine and 2% diaza-1,3-bicyclo[5.4.0]-undecane (DBU) in DMF for 10 min with argon bubbling as agitation. The final Fmoc deprotection as well as the acetyl protecting groups of sugar moiety were removed by 80% hydrazine hydrate (H<sub>2</sub>NNH<sub>2</sub>·H<sub>2</sub>O) in CH<sub>3</sub>OH with argon agitation 3× for 2 h. The glycopeptides were cleaved from the resin with a F<sub>3</sub>CCOOH/Et<sub>3</sub>SiH/H<sub>2</sub>O/PhOCH<sub>3</sub>/CH<sub>2</sub>Cl<sub>2</sub> (8:0.5:0.5:0.05:1) cocktail, which simultaneously removed the side chain protecting groups. The crude glycopeptides were precipitated in cold Et<sub>2</sub>O, redissolved in a minimal amount of distilled H<sub>2</sub>O, and then lyophilized. The crude glycopeptides were purified by RP-HPLC on a preparative C-18 Phenomenex (250 × 21.9 mm) column using CH<sub>3</sub>CN–H<sub>2</sub>O gradient system containing 0.1% CF<sub>3</sub>COOH. Homogeneity of the pure glycopeptides (≥95%) was confirmed by analytical RP-HPLC and high-resolution mass spectrometry.

**Receptor Binding Studies.** To determine the affinity and selectivity of the peptides for the  $\mu$ -,  $\delta$ -, and  $\kappa$ -opioid receptors, Chinese hamster ovary (CHO) cells that stably expressed one type of human opioid receptor were used as previously described.<sup>44</sup> Cell membranes were incubated at 25 °C with the radiolabeled ligands in a final volume of 1 mL of 50 mM Tris-HCl, pH 7.5. Incubation times of 60 min were used for the  $\mu$ -selective peptide [<sup>3</sup>H]DAMGO and the  $\kappa$ -selective ligand [<sup>3</sup>H]U69,593, and a 3 h incubation was used with the  $\delta$ -selective antagonist [<sup>3</sup>H]naltrindole. The final concentrations of [<sup>3</sup>H]DAMGO, [<sup>3</sup>H]naltrindole, and [<sup>3</sup>H]U69,593 were 0.25, 0.2, and 1 nM, respectively. Nonspecific binding was measured by inclusion of 10  $\mu$ M naloxone for the  $\mu$ - and  $\kappa$ -opioid receptors and 100  $\mu$ M naloxone for the  $\delta$ -opioid receptors. The binding was terminated by

filtering the samples through Schleicher & Scheuell no. 32 glass-fiber filters using a Brandel 48-well cell harvester. The filters were washed 3× with 3 mL of cold 50 mM Tris-HCl, pH 7.5, and were counted in 2 mL of ScintiSafe 30% scintillation fluid (Fisher Scientific, Fair Lawn, NJ). For [<sup>3</sup>H]U69,593 binding, the filters were soaked in 0.1% polyethylenimine for at least 30 min before use. Each experiment was performed in triplicate and included 12 different concentrations of the competing compound. Each experiment was repeated three times. IC<sub>50</sub> values were calculated by least-squares fit to a logarithm-probit analysis. *K<sub>i</sub>* values of unlabeled compounds were calculated from the equation  $K_i = (IC_{50})/(1 + S)$ , where *S* = (concentration of radioligand)/(*K<sub>d</sub>* of radioligand).<sup>45</sup>

**Circular Dichroism.** All circular dichroism (CD) spectra were obtained on OLIS DSM-20 automatic recording spectrophotometer equipped with temperature controller. The glycopeptide stock solutions were prepared by weighing the lyophilized powder using a Cahn/Ventron Instruments model 21 automatic analytical electrobalance. The samples were prepared by diluting the stock solution to 30  $\mu$ M. All CD spectra were the average of three scans recorded with baseline correction between 190 and 250 nm using an integration time of three seconds and a scan step of 0.5 nm in a cell with a path length of 0.1 cm at 20 °C. All spectra were smoothed by KaleidaGraph software (Synergy Software, USA). The molar ellipticities were calculated using the equation  $[\theta] = [\theta]_{\text{obs}}(\text{MRW})/10lC$ , where  $[\theta]_{\text{obs}}$  is the observed ellipticity in millidegrees, MRW is the mean residue weight, *l* is the cell path length in centimeters, and *C* is the glycopeptide concentration in milligrams per milliliter. The percent  $\alpha$ -helicity was determined using the equation % helix =  $[\theta]n \rightarrow p^*/-4000(1 - 2.5/n)/100$ , where *n* represents the number of amide bonds (including the C-terminal amide) in the glycopeptides and  $[\theta]n \rightarrow p^*$  is the molar ellipticity of the  $n \rightarrow p^*$  transition band at 222 nm.<sup>46</sup>

**NMR Spectroscopy.** All NMR spectra were obtained from a Bruker DRX600 600 MHz spectrometer. The concentration of glycopeptide samples for the NMR experiments varied from 2.5 to 3 mM. The micelle samples were prepared by dissolving the peptide and 50 equiv of perdeuterated SDS in 0.5 mL of phosphate buffer (10 mM)/D<sub>2</sub>O (9:1 ratio by volume). The acidity of the each sample was adjusted to pH 5.5 using NaOH as necessary. Internal standard 3-(trimethylsilyl)-*d*<sub>4</sub>-propionic acid (TSP) was added as a reference peak,  $\delta = 0$ . Rotating-frame Overhauser enhancement (ROESY),<sup>47</sup> nuclear Overhauser enhancement (NOESY), and total correlation spectra (TOCSY)<sup>48</sup> were acquired using standard pulse sequences and processed using XWINNMR (Bruker Inc.) and FELIX2000 (Accelrys Inc., San Diego, CA). Mixing times were 100 ms for TOCSY spectra and 300 ms for ROESY and NOESY spectra. All NMR experiments were 750 increments in *t*<sub>1</sub>, 24/32/32 scans each, and 1.5 s relaxation delay. The WATERGATE pulse sequence was employed to suppress the H<sub>2</sub>O/HOD signal.<sup>49</sup>

**Conformational Analysis.** Molecular distance constraints for the structure calculation were obtained from integral volumes of the ROESY or NOESY peaks with using software FELIX2000, and the NOE integral volumes were classified into strong, medium, and weak with 1.0, 2.5, and 3.5 Å as upper-bound distance. Molecular dynamics simulation was performed with the MOE software (Molecular Operating Environment, Chemical Computing Group, Canada) using a standard protocol available within the system.<sup>50</sup> Distance constraints are placed between protons identified through NMR-determined NOE-corresponding upper-boundary distances of 3 (strong), 4 (medium), and 5 Å (weak). A 25 kcal/mol energy penalty was used for the constraints. The structure was minimized initially using steepest descent followed by the conjugate gradient algorithm.

**Antinociceptive Potency and Efficacy Studies.** Adult male CD-1 mice (25–35 g) were obtained from Charles River Laboratories and housed in groups of 4 to 5 animals/cage. Animals were kept on a 12 h light–dark cycle (lights on 0700 h) with food and water available ad libitum until the time of formal testing/drug administration. They were maintained under standard housing conditions (temperature 22 ± 2 °C and relative humidity between 55 and 60%). All experimental procedures were approved by the University of New England Institutional Animal Care and Use Committee (IACUC) and were

conducted in compliance with the NIH Guide for the Care and Use of Laboratory Animals. The warm-water tail-flick assay was used to assess potency and efficacy of the test compounds. The assay used is a modified version<sup>51</sup> of the classic tail-flick test developed by D'Amour and Smith.<sup>52</sup> Mice were lightly but firmly grasped by the nape of the neck with the evaluators thumb and fingers, and the distal half of the tail was then dipped into a bath of circulating water thermostatically controlled at 55 °C (Neslab circulator). Latency to respond to the heat stimulus with a vigorous flexion of the tail was measured to the nearest 0.1 s. A baseline determination was made followed by testing at various times after drug injection (10, 20, 30, 45, 60, 90, and 120 min). A 10 s cutoff was used to prevent tissue damage to the tail. Antinociception was calculated by the following formula: % antinociception = [(test latency – baseline latency)/(10 – baseline latency)]100. For graphing purposes, mean and SEM values were calculated in Excel for each treatment group and time point. The  $A_{50}$  values and 95% confidence intervals (CI) were calculated using linear regression software from the dose–response curves (FlashCalc software; Dr. Michael Ossipov, University of Arizona, Tucson, AZ). Because latencies in this test are affected by tail skin temperature,<sup>53</sup> careful attention was paid to ensure that the ambient room temperature was maintained at 22 to 23 °C. All drugs were dissolved in distilled H<sub>2</sub>O for intracerebroventricular (i.c.v.) injections and in physiological saline (0.9% NaCl) for systemic injections. The i.c.v. injections were performed as previously described.<sup>54</sup> Briefly, mice were lightly anesthetized with ether, and a 5 mm incision was made along the midline of the scalp. An injection was made using a 25  $\mu$ L Hamilton syringe at a point 2 mm caudal and 2 mm lateral from bregma. All systemic injections were given in a volume based on the weight of the animal (0.1 mL/10 g bodyweight). For intravenous (i.v.) injections, mice were restrained in a Plexiglas holder, and the distal portion of the tail was dipped into 40 °C warm water for approximately 10 s to dilate the tail vein. The injection was made into the tail vein using a 30 gauge needle and a 1 mL syringe. Ten mice were used for each dose, i.c.v. and i.v., in order to construct dose–response curves.

## RESULTS

### Conformational Analysis by Circular Dichroism.

Because circular dichroism (CD) spectra reflect the peptide ensemble average of the alignment of the dipoles of the helix backbone, this simple but powerful technique can be used to obtain the secondary structures in both peptides and proteins quantitatively.<sup>55</sup> The CD spectra provide overall conformation but do not yield residue-specific information.<sup>56</sup> The helicity of the peptide sequences were measured in the three different solvent systems: H<sub>2</sub>O buffer, H<sub>2</sub>O/CF<sub>3</sub>CH<sub>2</sub>OH, and H<sub>2</sub>O/SDS micelles. See the Supporting Information for details of the CD data collection and interpretation.

In distilled H<sub>2</sub>O buffered to pH 5.5, the peptides and glycopeptides were largely unstructured. In the presence of SDS, the degree of helicity was as high as 57% for the glucosides (G1–G7) and mainly depended on the amino acids present in the address segment (Figure 2). Even higher helicities were observed for the unglycosylated peptides (U1–U7), the most helical of which (U1, 70%) was not soluble in water in the absence of SDS. The lactosides (L1–L7) were less helical than the glucosides (G1–G7). The highest helicities were observed with sequences bearing two helicogenic  $\alpha$ -aminoisobutyric acid (Aib) residues (U1, G1, and L1) and the lowest, sequences bearing two glycine residues in the address segment (U7, G7 and L7), with the alanine-bearing sequences showing intermediate helicities. In each case, increasing the degree of glycosylation (Ser[OH]  $\rightarrow$  Ser[ $\beta$ -Glc]  $\rightarrow$  Ser[ $\beta$ -Lact]) reduced the degree of helicity. However, the identity of the sugar moieties (glucoside vs lactoside) did not significantly affect the conformation of the micelle-bound glycopeptides,

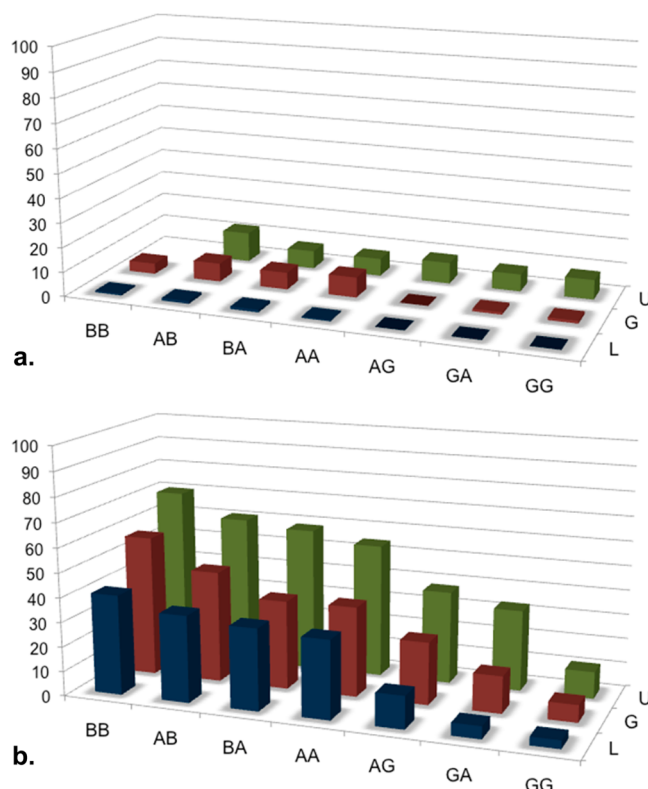


**Figure 2.** Helicity in the presence of H<sub>2</sub>O and SDS micelles. (a) Only small degrees of helicity (12% max) were observed in H<sub>2</sub>O buffer (pH 5.5) and only with the unglycosylated peptides, U. (b) In the presence of micelles, increased methylation at positions 9 and 12 in the address sequence (Gly  $\rightarrow$  Ala  $\rightarrow$  Aib) led to increased helicity (70% max). Increased glycosylation (-OH  $\rightarrow$  glucose  $\rightarrow$  lactose) led to reduced helicity.

causing only slight changes in the observed NOE's (see NMR results later). The CD spectra in the 30% TFE/H<sub>2</sub>O solvent mixture showed very similar trend as the micelle-bound compounds but with somewhat reduced helicities.

**Conformational Analysis by NMR.** Circular dichroism reflects general information on the overall molecular structure of glycopeptides in different solvents. In contrast, NMR spectroscopy is well-suited to study the local structure at a residue-specific level. All of the peptides and glycopeptides were characterized for their conformation in aqueous buffer and in deuterated SDS micelles (peptide/SDS  $\approx$  1:100) using 2D <sup>1</sup>H NMR (600 MHz). The spin systems were identified with TOCSY, and sequential assignments were made by the combined use of TOCSY and NOESY for experiments done in *d*<sub>2</sub>SDS/*D*<sub>2</sub>O/H<sub>2</sub>O and ROESY for experiments done in *D*<sub>2</sub>O/H<sub>2</sub>O. Although a few overlapping peaks were observed, unambiguous <sup>1</sup>H chemical shift assignments of all glycopeptides were completed on the basis of the sequential NOE measurements that were made, for example, *d*<sub>NN</sub> (*i*, *i* + 1), *d*<sub>αN</sub> (*i*, *i* + 1), and *d*<sub>βN</sub> (*i*, *i* + 1).<sup>57</sup> The complete chemical shift values of the amino acid residues and coupling constants for all glycopeptides are provided in the Supporting Information along with a complete description of the NMR experiments.

Proton chemical shift indices (CSI) for the  $\alpha$  positions were consistent with the helix assignments made by NOE data.<sup>58</sup> The observed chemical shift differences between the ideal helix and random coil CSI values expected and the observed CSI values were consistent with the CD data for each molecule.

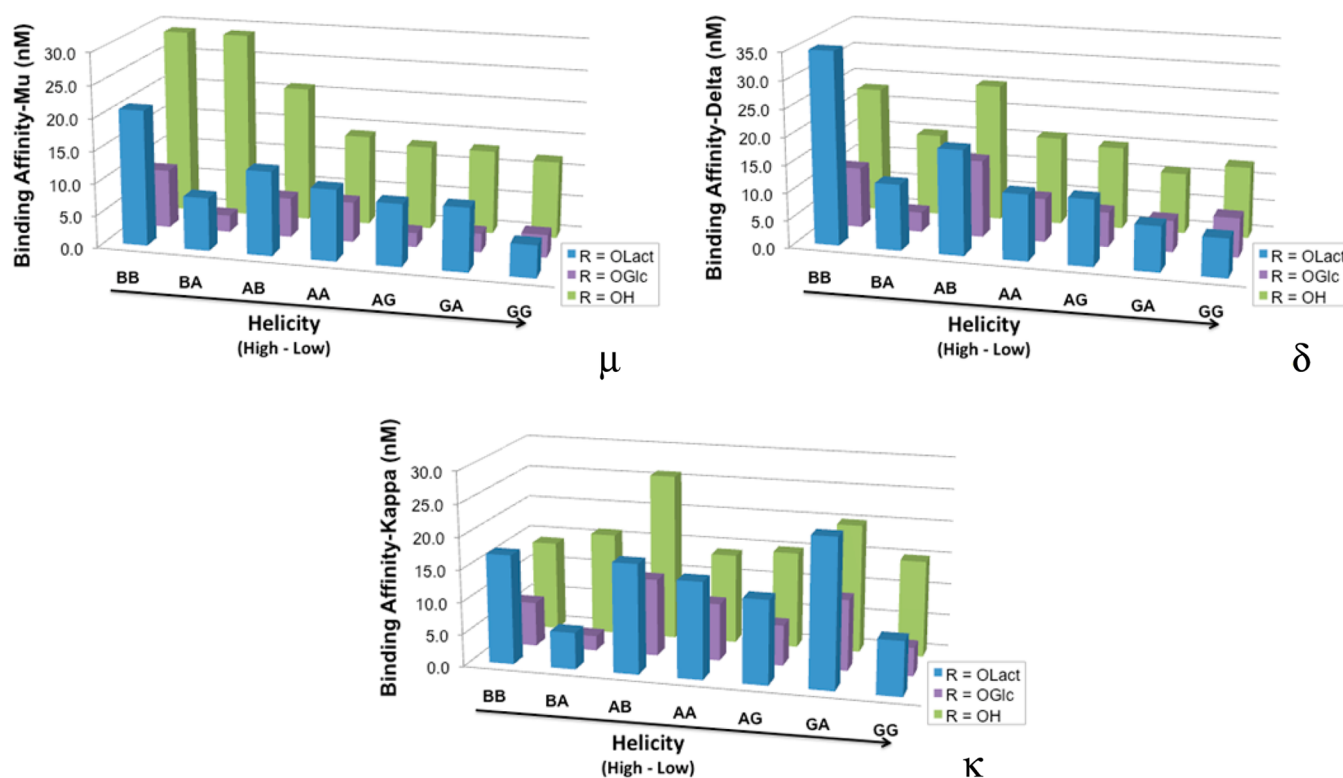


**Figure 3.** Opioid binding.<sup>46,47</sup> Binding was determined in membranes from Chinese hamster ovary (CHO) cells that stably expressed either the human  $\mu$ -,  $\kappa$ -, or  $\delta$ -opioid receptors. Each membrane preparation was incubated with 12 different concentrations of each peptide/glycopeptide. Each measurement was performed in triplicate, and each experiment was replicated three times.

**Table 2.** Opioid Receptor Binding Determined by Radioligand Displacement in Membrane Preparations with hMOR, hDOR, and hKOR Receptors Expressed in CHO Cells<sup>45,46</sup>

helix series	1 ~B~B~	2 ~A~B~	3 ~B~A~	4 ~A~A~	5 ~A~G~	6 ~G~A~	7 ~G~G~	S°
$\mu$ -Binding ( $K_i$ 's in nM) vs [ $^3$ H]DAMGO								
L	21 $\pm$ 0.90	8.2 $\pm$ 0.60	13 $\pm$ 0.54	11 $\pm$ 1.4	9.6 $\pm$ 0.18	9.8 $\pm$ 0.97	5.0 $\pm$ 0.37	S**
G	9.1 $\pm$ 0.39	2.6 $\pm$ 0.29	6.1 $\pm$ 0.31	6.2 $\pm$ 0.47	2.2 $\pm$ 0.30	2.9 $\pm$ 0.32	3.5 $\pm$ 0.55	S*
U	29 $\pm$ 3.1	29 $\pm$ 0.67	21 $\pm$ 2.6	14 $\pm$ 2.3	13 $\pm$ 0.97	13 $\pm$ 1.2	12 $\pm$ 1.8	S
$\delta$ -Binding ( $K_i$ 's in nM) vs [ $^3$ H]naltrindole								
L	35 $\pm$ 3.0	12 $\pm$ 0.94	19 $\pm$ 0.67	12 $\pm$ 0.99	12 $\pm$ 1.0	8.2 $\pm$ 0.29	7.0 $\pm$ 0.57	S**
G	11 $\pm$ 1.2	3.6 $\pm$ 0.23	14 $\pm$ 2.1	7.9 $\pm$ 1.0	6.3 $\pm$ 0.094	5.7 $\pm$ 0.35	7.1 $\pm$ 1.0	S*
U	23 $\pm$ 2.8	15 $\pm$ 0.79	25 $\pm$ 1.6	16 $\pm$ 1.9	15 $\pm$ 0.98	11 $\pm$ 0.91	13 $\pm$ 2.2	S
$\kappa$ -Binding ( $K_i$ 's in nM) vs [ $^3$ H]U69,593								
L	17 $\pm$ 1.9	5.7 $\pm$ 0.13	17 $\pm$ 1.6	15 $\pm$ 0.39	13 $\pm$ 0.76	23 $\pm$ 2.3	8.4 $\pm$ 1.2	S**
G	6.9 $\pm$ 0.58	2.3 $\pm$ 0.31	12 $\pm$ 0.94	8.9 $\pm$ 1.0	6.3 $\pm$ 0.41	11 $\pm$ 0.26	4.4 $\pm$ 0.47	S*
U	14 $\pm$ 1.4	16 $\pm$ 0.16	26 $\pm$ 1.6	14 $\pm$ 2.1	15 $\pm$ 1.3	20 $\pm$ 1.4	15 $\pm$ 1.9	S

Almost all of the  $\alpha$ CH resonances showed negative deviations except for residues Leu<sup>S</sup> and Ser.<sup>15</sup> This trend was observed for all the glycopeptides; however, it should be noted that there is no random-coil reference standard available for glycosylated serine. However, it seems reasonable to make a qualitative comparison of helix content between closely related peptides.

Methods described by Gierasch and co-workers<sup>59</sup> were applied. First, the average conformational shift was calculated for each peptide by adding all upfield shifts in the helical regions and dividing by the total number of peptide bonds. Then, to obtain the overall helical contents for each peptide, the average conformational shift was divided by 0.35 ppm, which was assigned for 100% helicity. Because there are no random-coil values available for the serine glycosides<sup>60</sup> and  $\alpha$ -

amino isobutyric acid has no  $\alpha$ -protons, these residues were not included in the calculation.

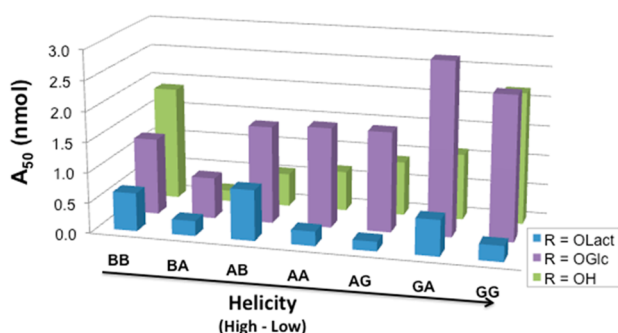
All of the peptide backbones exhibited strong consecutive  $d_{\alpha N}(i, i + 1)$  NOEs in H<sub>2</sub>O/D<sub>2</sub>O and in the presence of SDS micelles. Unlike what was observed in H<sub>2</sub>O/D<sub>2</sub>O, a continuous stretch of sequential, strong  $d_{NN}(i, i + 1)$  NOEs were observed throughout all sequences in the presence of SDS micelles. In H<sub>2</sub>O/D<sub>2</sub>O, the  $d_{NN}(i, i + 1)$  NOEs were too weak to be observed, and no other long-range NOEs were observable, suggesting that random-coil conformational ensembles exist in this solvent, as suggested by the CD data, or only nascent helix formation at best. CD reflects an instantaneous snapshot of the entire ensemble, whereas the nuclear Overhauser effects (NOEs) take 50–100  $\mu$ s to build, depending on the peptide backbone to hold a particular conformation for a relatively long



period of time. Thus, the helical content obtained by NMR for a typical case, glycopeptide **G1** ( $\beta$ -glucoside), was less than 20% of CD results. Because the NOEs were obtained by true NOESY experiments (not ROESY), the NMR structures are biased toward the more static, micelle-bound structures at the expense of the more dynamic, random-coil structures found in solution. Thus, the NMR data is useful insofar as it confirms the existence of helices, but it is not useful for quantifying the degree of helicity, which is more reliably predicted by the CD experiments.

**Receptor Binding Studies.** The peptides (**U1–U7**) and glycopeptides (**L1–L7** and **G1–G7**) all showed low nanomolar affinities (Figure 3 and Table 2) for the three classical opioid receptor subtypes,  $\mu$  (hMOR),  $\delta$  (hDOR), and  $\kappa$  (hKOR), using published methods.<sup>61</sup>

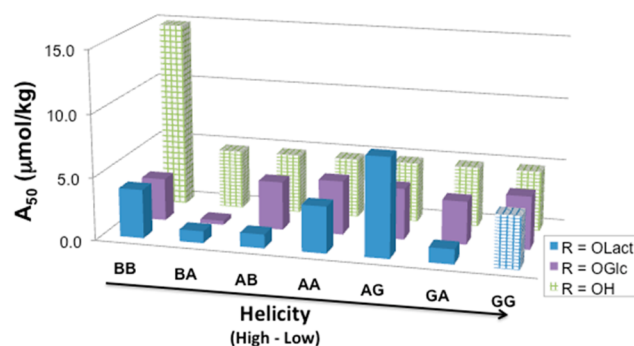
**In Vivo Antinociception.** Figures 4 and 5 include the  $A_{50}$  values of each peptide in the 55 °C tail-flick test following i.c.v.



Linker Address		$A_{50}$ Values, nmol (95% Confidence Intervals)		
		R = OLact	R = OGlc	R = OH
Helicity (Low → High)	BB	0.63 (0.51-0.78)	1.27 (0.59-2.9)	1.89 (1.4-2.7)
	BA	0.25 (0.19-0.32)	0.68 (0.50-0.92)	0.18 (0.14-0.25)
	AB	0.84 (0.71-0.98)	1.61 (0.8-3.0)	0.55 (0.32-0.95)
	AA	0.24 (0.19-0.31)	1.66 (0.93-2.9)	0.66 (0.50-0.87)
	AG	0.16 (0.15-0.17)	1.66 (1.0-2.8)	0.90 (0.64-1.3)
	GA	0.59 (0.44-0.81)	2.87 (1.5-5.5)	1.10 (0.50-2.4)
	GG	0.26 (0.21-0.33)	2.39 (1.7-3.4)	2.19 (1.6-3.0)

**Figure 4.** Potency estimates after i.c.v. administration. Mouse tail-flick studies were performed at 55 °C. The vertical axis ( $A_{50}$  values) is marked in nanomoles per mouse. The  $A_{50}$  values were calculated using linear regression software (FlashCalc), and 95% confidence intervals are included in the table.

or i.v. administration. All compounds were full and potent agonists following i.c.v. administration, with  $A_{50}$  values falling in the 0.1–2.5 nmol/mouse range. The lactosylated peptides tended to be more potent than both the glucosylated and unglycosylated compounds, with  $A_{50}$  scores ranging between 0.1 and 0.9 nmol/mouse (Figure 4). Peptide  $A_{50}$  values following i.v. administration displayed more variability than those obtained from i.c.v. administration. The unglycosylated peptides failed to produce >20% antinociception following i.v. administration in the 55 °C tail-flick assay at the doses tested (10 or 32 mg/kg, Figure 5). In contrast, most of the glycosylated analogues produced potent full-agonist effects, with  $A_{50}$  values for the disaccharides ranging from <1 to 5.3  $\mu$ mol/kg. The one exception was **L7** (lactosylated GG), which produced <40% antinociception at 32 mg/kg. Higher doses of **L7** were not tested because there were insufficient amounts of



Linker Address		$A_{50}$ Values, $\mu$ mol/Kg (95% Confidence Intervals)		
		R = OLact	R = OGlc	R = OH
Helicity (Low → High)	BB	3.89 (3.0-5.1)	3.39 (2.6-4.5)	>14.9 (n/a)
	BA	0.96 (0.67-1.4)	0.32 (0.24-4.2)	>4.72 (n/a)
	AB	1.11 (0.93-1.33)	3.86 (3.0-5.0)	>4.75 (n/a)
	AA	3.71 (2.6-5.3)	4.30 (3.3-5.7)	>4.75 (n/a)
	AG	7.91 (5.3-11.8)	4.07 (2.9-5.8)	>4.78 (n/a)
	GA	1.19 (0.88-1.6)	3.43 (2.6-4.5)	>4.78 (n/a)
	GG	>4.16 (n/a)	4.21 (3.0-5.9)	>4.81 (n/a)

**Figure 5.** Potency estimates after i.v. administration. Mouse tail-flick studies were performed at 55 °C. The vertical axis is marked in  $\mu$ mol/kg. The  $A_{50}$  values were calculated using linear regression software (FlashCalc), and 95% confidence intervals are included in the table. Note that the checked bars indicate maximum doses tested, not  $A_{50}$  values. No significant antinociception was observed for the unglycosylated peptides nor for the least helical lactoside (GG).

compound available. The role of multiple receptor subtype activation<sup>62</sup> is not considered here.

## DISCUSSION

It was hypothesized that modulation of membrane affinity (via alterations in the degree of amphipathicity) is important for BBB penetration rates,<sup>30</sup> for drug distribution properties,<sup>21</sup> and for receptor affinity.<sup>63</sup> The amphipathic character of the helix can facilitate a drug or hormone to bind its specific receptor by narrowing the receptor search from an inefficient 3D search of the extracellular milieu to a much more rapidly converging 2D search along the membrane surface. Second, membrane insertion of the helical address might allow the pharmacophore or message to be fixed in a specific geometry relative to the membrane.<sup>64</sup> It is known that simply producing highly amphipathic sequences is insufficient to facilitate systemic delivery and penetration of the BBB.<sup>21b</sup>

The  $\alpha$ -methylation of amino acids is well-known to stabilize helix formation<sup>8,65</sup> and was used to produce a series of helical address regions with increasing intrinsic stability by increasing methylation (glycine  $\rightarrow$  alanine  $\rightarrow$   $\alpha$ -aminoisobutyric acid). In all three series of opioid agonists, **U1–7**, **G1–7**, and **L1–7** (unglycosylated, glucosylated, and lactosylated, respectively), the CD and NMR data showed increasing helicity in the presence of TFE or SDS. Increasing glycosylation (no sugar  $\rightarrow$  glycoside  $\rightarrow$  lactoside) decreased the observed helicity in every case. We hypothesize that this occurs not because the helix is destabilized but by further stabilizing the random-coil structures by increasing their water solubility. Although we can gauge the overall ratio of bound versus unbound helices, we do not know the on and off rates for the helix–micelle binding event (a surrogate for helix–membrane binding). It would be surprising if these rates were not affected by the glycosylation state. We

hypothesize that the glycopeptides gain entry to the CNS by transcytosis at the BBB and that a minimal level of membrane interaction (residence time?) is required for efficient BBB penetration. It is tempting to speculate that increased rates of membrane adsorption–desorption might lead to enhanced BBB penetration rates, either by affecting the biophysics of the initial endocytotic event or by promoting subsequent endosomal escape of the glycopeptides.

On the basis of the receptor binding results and intracerebroventricular (i.c.v.) (Figure 4) and intravenous (i.v.) tail-flick studies (Figure 5), only the glucoside **G3** (BA) displayed somewhat greater receptor binding affinity and in vivo potency compared to the compounds that had similar bioactivities. On the basis of the i.v.  $A_{50}$  value calculations, the compound presumably exhibited efficient penetration across the BBB in mice. All lactosides (L series) had higher binding affinities with  $\mu$ -,  $\delta$ -, and  $\kappa$ -receptors than the corresponding glucosides (G series) after i.c.v. injection. Nevertheless, the more flexible lactoside **L7** (GG) could not, apparently, cross the BBB at all after i.v. injection. (Figure 5). On the basis of the i.c.v. results, the lactosides were 2–10 times more potent than the glucosides, presumably because of increased water solubility within the CNS. Compared to tail flick results after i.v. injection, the more hydrophilic peptide **L2** was  $\sim 3$  times more potent than peptide **G2**, but **L3** showed similar potency to **G3** after peripheral administration. Lactoside **L7** with random-coil conformations in TFE and SDS micelles likely does not penetrate the BBB after i.v. injection, even though the compound has a greater antinociceptive potency than **G7** after i.c.v. injection. Presumably, it is too water-soluble and does not bind to membranes strongly enough to undergo endocytosis to penetrate the BBB. None of the unglycosylated peptides showed antinociceptive properties when administered peripherally (Figure 5).

## CONCLUSIONS

All of the glycopeptides and peptides had relatively high affinity for the three cloned opioid receptors, (Table 2) and displayed good in vivo antinociception following i.c.v. administration (Figure 4). Not all of the glycopeptides showed good activity after peripheral administration by i.v. injection (Figure 5). This supports earlier conclusions that glycosylation of smaller enkephalin-based peptides<sup>21a,44,45</sup> increases bioactivities and penetration of the BBB.<sup>19,20</sup> Both CD and NMR studies confirmed that all the glycopeptides displayed random-coil conformational ensembles in aqueous solution and increasing degrees of helicity in TFE and SDS solution predicted by increasing substitution of residues 9 and 12, Gly  $\rightarrow$  Ala  $\rightarrow$  Aib.<sup>8,21,30,34,66</sup> If there were no helix-destabilizing glycine residues on the address segment, then glycopeptides showed clear amphipathic  $\alpha$ -helical structures by CD and by NMR. None of the unglycosylated peptides showed antinociceptive properties when administered peripherally (Figure 5). The helix of peptide **U1** was so stable that it was not even soluble in aqueous media in the absence of SDS.

The results suggest that simply introducing highly helical sequences on the address segment is not by itself sufficient to promote stability and penetration of the BBB. It is hypothesized that the helix must also be capable of assuming a water-soluble random-coil conformation and that the energy barrier between random coil and helical states must be low enough to permit rapid interconversion between the two states; this characteristic was termed bioussian, denoting two (bi) essences (ousia), a

water-soluble conformational ensemble and a membrane-bound conformation.<sup>30</sup> The bioussian nature of a glycopeptide permits high-affinity receptor binding, allows membrane hopping to impart drug-like characteristics, and promotes penetration of the BBB. This is confirmed by comparing glucoside **G2** and lactoside **L2** (Table 2). The CD spectra of **G2** indicates a strong helix but a relatively low affinity for opioid receptors and a weak penetration of the BBB. The increased hydrophilicity of the lactose-bearing **L2** (decreased energy barrier between random coil and helical states) allows **L2** to bind more strongly than **G2** and to penetrate the BBB after i.v. injection. Unglycosylated peptide **U1** showed excellent opioid binding, yet it was less antinociceptive than **U2** or **U3** after i.c.v. administration (Figure 4) and was not water-soluble in the absence of SDS. Further studies with other opioid messages (e.g.,  $\mu$ - and  $\delta$ -selective agonists) and replacement of the linkage element L-proline with more flexible linkers will be discussed elsewhere.

## ASSOCIATED CONTENT

### Supporting Information

Experimental details for the synthesis, HPLC, MS, NMR, and CD of the peptides and glycopeptides. This material is available free of charge via the Internet at <http://pubs.acs.org>.

## AUTHOR INFORMATION

### Corresponding Author

\*E-mail: [poltt@u.arizona.edu](mailto:poltt@u.arizona.edu); Phone: (520) 370-2654.

### Notes

The authors declare no competing financial interest.

## ACKNOWLEDGMENTS

We thank the Office of Naval Research (N00014-05-1-0807 and N00014-02-1-0471), the National Science Foundation (CHE-9526909), the National Institute of Neurological Disorders and Stroke (R01NS52727), and the National Institute of General Medical Sciences (P20 GM103643-01A1) for financial support. In addition, the expert technical assistance of Drs. Lajos Szabó (HPLC analyses) and Chad Park (CD measurements) is gratefully acknowledged.

## ABBREVIATIONS USED

TFE, trifluoroethanol;  $A_{50}$ , analgesic potency (50% activity in the 55 °C mouse tail-flick assay)

## REFERENCES

- (1) Brasnjevic, I.; Steinbusch, H. W. M.; Schmitz, C.; Martinez-Martinez, P. Delivery of peptide and protein drugs over the blood-brain barrier. *Prog. Neurobiol.* **2009**, *87*, 212–251.
- (2) Hughes, J.; Smith, T. W.; Kosterlitz, H. W.; Fothergill, L. A.; Morgan, B. A.; Morris, H. R. Identification of two related pentapeptides from the brain with potent opiate agonist activity. *Nature* **1975**, *258*, 577–580.
- (3) (a) Adessi, C.; Soto, C. Converting a peptide into a drug: Strategies to improve stability and bioavailability. *Curr. Med. Chem.* **2002**, *9*, 963–978. (b) *Peptide and Protein Delivery*; Van der Walle, C., Ed.; Academic Press: London, 2011.
- (4) Witt, K.; Davis, T. CNS drug delivery: Opioid peptides and the blood-brain barrier. *AAPS J.* **2006**, *8*, E76–E88.
- (5) del Zoppo, G. J. Stroke and neurovascular protection. *New Engl. J. Med.* **2006**, *354*, 553–555.
- (6) Mercadante, S.; Arcuri, E. Delivery of opioid analgesics to the brain: The role of blood-brain barrier. *Gene Ther. Mol. Biol.* **2009**, *13A*, 82–90.



- (7) Habgood, M. D.; Begley, D. J.; Abbott, N. J. Determinants of passive drug entry into the central nervous system. *Cell. Mol. Neurobiol.* **2000**, *20*, 231–253.
- (8) Polt, R.; Dhanasekaran, M.; Keyari, C. Glycosylated neuropeptides: A new vista for neuropsychopharmacology? *Med. Res. Rev.* **2005**, *25*, 557–585.
- (9) Hansen, D. W.; Stapelfeld, A.; Savage, M. A.; Reichman, M.; Hammond, D. L.; Haaseth, R. C.; Mosberg, H. I. Systemic analgesic activity and delta-opioid selectivity in [2,6-dimethyl-Tyr<sup>1</sup>,D-Pen<sup>5</sup>]enkephalin. *J. Med. Chem.* **1992**, *35*, 684–687.
- (10) Bewley, T. A.; Li, C. H. Evidence for tertiary structure in aqueous-solutions of human beta-endorphin as shown by difference absorption-spectroscopy. *Biochemistry* **1983**, *22*, 2671–2675.
- (11) (a) Jakas, A.; Horvat, S. The effect of glycation on the chemical and enzymatic stability of the endogenous opioid peptide, leucine-enkephalin, and related fragments. *Bioorg. Chem.* **2004**, *32*, 516–526. (b) Poduslo, J. F.; Curran, G. L. Glycation increases the permeability of proteins across the blood nerve and blood-brain barriers. *Mol. Brain Res.* **1994**, *23*, 157–162.
- (12) (a) Tsuji, A.; Tamai, I. Carrier-mediated or specialized transport of drugs across the blood-brain barrier. *Adv. Drug Delivery Rev.* **1999**, *36*, 277–290. (b) Begley, D. J. The blood-brain barrier: Principles for targeting peptides and drugs to the central nervous system. *J. Pharm. Pharmacol.* **1996**, *48*, 136–146.
- (13) Ghosh, M. K.; Mitra, A. K. Brain parenchymal metabolism of 5-iodo-2'-deoxyuridine and 5'-ester prodrugs. *Pharm. Res.* **1992**, *9*, 1048–1052.
- (14) Bickel, U.; Kang, Y. S.; Pardridge, W. M. In-vivo cleavability of a disulfide-based chimeric opioid peptide in rat-brain. *Bioconj. Chem.* **1995**, *6*, 211–218.
- (15) Chakrabarti, S.; Sima, A. A. F. The presence of anionic sites in basement-membranes of cerebral capillaries. *Microvasc. Res.* **1990**, *39*, 123–127.
- (16) Tosi, G.; Costantino, L.; Ruozi, B.; Forni, F.; Vandelli, M. A. Polymeric nanoparticles for the drug delivery to the central nervous system. *Expert Opin. Drug Delivery* **2008**, *5*, 155–174.
- (17) Powell, M. F.; Stewart, T.; Otvos, L.; Urge, L.; Gaeta, F. C. A.; Sette, A.; Arrhenius, T.; Thomson, D.; Soda, K.; Colon, S. M. Peptide stability in drug development 0.2. Effect of single amino-acid substitution and glycosylation on peptide reactivity in human serum. *Pharm. Res.* **1993**, *10*, 1268–1273.
- (18) Fisher, J. F.; Harrison, A. W.; Bundy, G. L.; Wilkinson, K. F.; Rush, B. D.; Ruwart, M. J. Peptide to glycopeptide - glycosylated oligopeptide renin inhibitors with attenuated in vivo clearance properties. *J. Med. Chem.* **1991**, *34*, 3140–3143.
- (19) Egleton, R. D.; Mitchell, S. A.; Huber, J. D.; Janders, J.; Stropova, D.; Polt, R.; Yamamura, H. I.; Hruby, V. J.; Davis, T. P. Improved bioavailability to the brain of glycosylated Met-enkephalin analogs. *Brain Res.* **2000**, *881*, 37–46.
- (20) Egleton, R. D.; Mitchell, S. A.; Huber, J. D.; Palian, M. M.; Polt, R.; Davis, T. P. Improved blood-brain barrier penetration and enhanced analgesia of an opioid peptide by glycosylation. *J. Pharm. Exp. Ther.* **2001**, *299*, 967–972.
- (21) (a) Palian, M. M.; Boguslavsky, V. I.; O'Brien, D. F.; Polt, R. Glycopeptide-membrane interactions: Glycosyl enkephalin analogues adopt turn conformations by NMR and CD in amphipathic media. *J. Am. Chem. Soc.* **2003**, *125*, 5823–5831. (b) Dhanasekaran, M.; Palian, M.; Alves, I.; Yeomans, L.; Keyari, C.; Davis, P.; Bilsky, E.; Egleton, R.; Yamamura, H.; Jacobsen, N.; Tollin, G.; Hruby, V.; Porreca, F.; Polt, R. Glycopeptides related to beta-endorphin adopt helical amphipathic conformations in the presence of lipid bilayers. *J. Am. Chem. Soc.* **2005**, *127*, 5435–5448.
- (22) (a) Suzuki, K.; Susaki, H.; Okuno, S.; Yamada, H.; Watanabe, H. K.; Sugiyama, Y. Specific renal delivery of sugar-modified low-molecular-weight peptides. *J. Pharm. Exp. Ther.* **1999**, *288*, 888–897. (b) Suzuki, K.; Susaki, H.; Okuno, S.; Sugiyama, Y. Renal drug targeting using a vector "alkylglycoside". *J. Pharm. Exp. Ther.* **1999**, *288*, 57–64.
- (23) Gysin, B.; Schwyzler, R. Head group and structure specific interactions of enkephalins and dynorphin with liposomes – investigation by hydrophobic photolabeling. *Arch. Biochem. Biophys.* **1983**, *225*, 467–474.
- (24) Taylor, J. W.; Kaiser, E. T. Opioid receptor selectivity of peptide models of beta-endorphin. *Int. J. Pept. Protein Res.* **1989**, *34*, 75–80.
- (25) Taylor, J. W.; Miller, R. J.; Kaiser, E. T. Characterization of an amphiphilic helical structure in beta-endorphin through the design, synthesis, and study of model peptides. *J. Biol. Chem.* **1983**, *258*, 4464–4471.
- (26) Taylor, J. W.; Miller, R. J.; Kaiser, E. T. Structural characterization of beta-endorphin through the design, synthesis, and study of model peptides. *Mol. Pharmacol.* **1982**, *22*, 657–666.
- (27) Taylor, J. W.; Osterman, D. G.; Miller, R. J.; Kaiser, E. T. Design and synthesis of a model peptide with beta-endorphin-like properties. *J. Am. Chem. Soc.* **1981**, *103*, 6965–6966.
- (28) Zhang, C. W.; Miller, W.; Valenzano, K. J.; Kyle, D. J. Novel, potent ORL-1 receptor agonist peptides containing alpha-helix-promoting conformational constraints. *J. Med. Chem.* **2002**, *45*, 5280–5286.
- (29) Krishnadas, A.; Onyuskel, H.; Rubinstein, I. Interactions of VIP, secretin and PACAP(1–38) with phospholipids: A biological paradox revisited. *Curr. Pharm. Des.* **2003**, *9*, 1005–1012.
- (30) Egleton, R. D.; Bilsky, E. J.; Tollin, G.; Dhanasekaran, M.; Lowery, J.; Alves, I.; Davis, P.; Porreca, F.; Yamamura, H. I.; Yeomans, L.; Keyari, C. M.; Polt, R. Biosynthetic glycopeptides penetrate the blood-brain barrier. *Tetrahedron: Asymmetry* **2005**, *16*, 65–75.
- (31) Buck, M. Trifluoroethanol and colleagues: Cosolvents come of age. Recent studies with peptides and proteins. *Q. Rev. Biophys.* **1998**, *31*, 295–355.
- (32) Cornette, J. L.; Cease, K. B.; Margalit, H.; Spouge, J. L.; Berzofsky, J. A.; Delisi, C. Hydrophobicity scales and computational techniques for detecting amphipathic structures in proteins. *J. Mol. Biol.* **1987**, *195*, 659–685.
- (33) (a) Adam, G.; Delbruck, M. Reduction of dimensionality in biological diffusion processes. In *Structural Chemistry and Molecular Biology*; Rich, A., Davidson, N., Eds.; W. H. Freeman: San Francisco, CA, 1968; pp 198–215. (b) Taylor, J. W.; Kaiser, E. T. The structural characterization of  $\beta$ -endorphin and related peptide hormones and neurotransmitters. *Pharm. Rev.* **1986**, *38*, 291–319.
- (34) Lowery, J. J.; Yeomans, L.; Keyari, C. M.; Davis, P.; Porreca, F.; Knapp, B. I.; Bidlack, J. M.; Bilsky, E. J.; Polt, R. Glycosylation improves the central effects of DAMGO. *Chem. Biol. Drug Des.* **2007**, *69*, 41–47.
- (35) Varamini, P.; Mansfeld, F. M.; Blanchfield, J. T.; Wyse, B. D.; Smith, M. T.; Toth, I. Synthesis and biological evaluation of an orally active glycosylated endomorphin-1. *J. Med. Chem.* **2012**, *55*, 5859–5867.
- (36) Segrest, J. P.; Deloof, H.; Dohlman, J. G.; Brouillette, C. G.; Anantharamaiah, G. M. Amphipathic helix motif – classes and properties. *Proteins: Struct., Funct., Genet.* **1990**, *8*, 103–117.
- (37) Shai, Y. Mechanism of the binding, insertion and destabilization of phospholipid bilayer membranes by  $\alpha$ -helical antimicrobial and cell non-selective membrane-lytic peptides. *Biochim. Biophys. Acta* **1999**, *1462*, 55–70.
- (38) (a) Costantini, S.; Colonna, G.; Facchiano, A. M. Amino acid propensities for secondary structures are influenced by the protein structural class. *Biochem. Biophys. Res. Commun.* **2006**, *342*, 441–451. (b) Wako, H.; Blundell, T. L. Use of amino-acid environment-dependent substitution tables and conformational propensities in structure prediction from aligned sequences of homologous proteins 0.2. Secondary structures. *J. Mol. Biol.* **1994**, *238*, 693–708.
- (39) (a) Su, J. Y.; Hodges, R. S.; Kay, C. M. Effect of chain-length on the formation and stability of synthetic alpha-helical coiled coils. *Biochemistry* **1994**, *33*, 15501–15510. (b) Kinnear, B. S.; Hartings, M. R.; Jarrold, M. F. Helix unfolding in unsolvated peptides. *J. Am. Chem. Soc.* **2001**, *123*, 5660–5667.

- (40) Seibel, J.; Hillringhaus, L.; Moraru, R. Microwave-assisted glycosylation for the synthesis of glycopeptides. *Carbohydr. Res.* **2005**, *340*, 507–511.
- (41) Keyari, C. M.; Polt, R. Serine and threonine schiff base esters react with beta-anomeric peracetates in the presence of  $\text{BF}_3 \cdot \text{Et}_2\text{O}$  to produce  $\beta$ -glycosides. *J. Carbohydr. Chem.* **2010**, *29*, 181–206.
- (42) Lefever, M. R.; Szabò, L. Z.; Anglin, B.; Ferracane, M.; Hogan, J.; Cooney, L.; Polt, R. Glycosylation of  $\alpha$ -amino acids by sugar acetate donors with  $\text{InBr}_3$ . Minimally competent Lewis acids. *Carbohydr. Res.* **2012**, *351*, 121–125.
- (43) Coss, C.; Carrocci, T.; Maier, R. M.; Pemberton, J. E.; Polt, R. Minimally competent lewis acid catalysts: Indium(III) and bismuth(III) salts produce rhamnosides (=6-deoxymannosides) in high yield and purity. *Helv. Chim. Acta* **2012**, *95*, 2652–2659.
- (44) Polt, R.; Szabò, L. Z.; Treiberg, J.; Li, Y.; Hruby, V. J. General methods for  $\alpha$ - or  $\beta$ -O-Ser/Thr glycosides and glycopeptides. Solid-phase synthesis of O-glycosyl cyclic enkephalin analogues. *J. Am. Chem. Soc.* **1992**, *114*, 10249–10258.
- (45) Mitchell, S. A.; Pratt, M. R.; Hruby, V. J.; Polt, R. Solid-phase synthesis of O-linked glycopeptide analogues of enkephalin. *J. Org. Chem.* **2001**, *66*, 2327–2342.
- (46) Parkhill, A. L.; Bidlack, J. M. Several  $\delta$ -opioid receptor ligands display no subtype selectivity to the human  $\delta$ -opioid receptor. *Eur. J. Pharmacol.* **2002**, *451*, 257–264.
- (47) Cheng, Y. C.; Prusoff, W. H. Relationship between the inhibition constant ( $K_i$ ) and the concentration of inhibitor which causes 50% inhibition (150) of an enzymatic reaction. *Biochem. Pharmacol.* **1973**, *22*, 3099–3108.
- (48) Scholtz, J. M.; Marqusee, S.; Baldwin, R. L.; York, E. J.; Stewart, J. M.; Santoro, M.; Bolen, D. W. Calorimetric determination of the enthalpy change for the alpha-helix to coil transition of an alanine peptide in water. *Proc. Natl. Acad. Sci. U.S.A.* **1991**, *88*, 2854–2858.
- (49) Rance, M. Improved techniques for homonuclear rotating-frame and isotropic mixing experiments. *J. Magn. Reson.* **1987**, *74*, 557–564.
- (50) Davis, D. G.; Bax, A. Assignment of complex  $^1\text{H}$  NMR spectra via two-dimensional homonuclear Hartmann-Hahn spectroscopy. *J. Am. Chem. Soc.* **1985**, *107*, 2820–2821.
- (51) Piotto, M.; Saudek, V.; Sklenar, V. Gradient-tailored excitation for single-quantum nmr-spectroscopy of aqueous-solutions. *J. Biomol. NMR* **1992**, *2*, 661–665.
- (52) Ogawa, H.; Nakano, M.; Watanabe, H.; Starikov, E. B.; Rothstein, S. M.; Tanaka, S. Molecular dynamics simulation study on the structural stabilities of polyglutamine peptides. *Comput. Biol. Chem.* **2008**, *32*, 102–110.
- (53) Janssen, P. A. J.; Niemegeers, C. J. C.; Dony, J. G. H. Inhibitory effect of fentanyl and other morphine-like analgesics on warm water induced tail withdrawal reflex in rats. *Arzneim. Forsch.* **1963**, *13*, 502–ff.
- (54) D'Amour, F. E.; Smith, D. L. A method for determining loss of pain sensation. *J. Pharm. Exp. Ther.* **1941**, *72*, 74–79.
- (55) Hole, K.; Tjolsen, A. The tail-flick and formalin tests in rodents – changes in skin temperature as a confounding factor. *Pain* **1993**, *53*, 247–254.
- (56) Porreca, F.; Mosberg, H. I.; Hurst, R.; Hruby, V. J.; Burks, T. F. Roles of mu-receptors, delta-receptors and kappa-opioid receptors in spinal and supraspinal mediation of gastrointestinal transit effects and hot-plate analgesia in the mouse. *J. Pharm. Exp. Ther.* **1984**, *230*, 341–348.
- (57) Woody, R. W. Circular dichroism. *Methods Enzymol.* **1995**, *246*, 34–71.
- (58) Merutka, G.; Morikis, D.; Bruschweiler, R.; Wright, P. E. NMR evidence for multiple conformations in a highly helical model peptide. *Biochemistry* **1993**, *32*, 13089–13097.
- (59) Wuthrich, K. *NMR of Proteins and Nucleic Acids*; Wiley Press: New York, 1986.
- (60) Merutka, G.; Dyson, H. J.; Wright, P. E. Random coil  $^1\text{H}$  chemical-shifts obtained as a function of temperature and trifluoroethanol concentration for the peptide series GGXGG. *J. Biomol. NMR* **1995**, *5*, 14–24.
- (61) Rizo, J.; Blanco, F. J.; Kobe, B.; Bruch, M. D.; Gierasch, L. M. Conformational behavior of *Escherichia coli* OmpA signal peptides in membrane mimetic environments. *Biochemistry* **1993**, *32*, 4881–4894.
- (62) Palian, M. M.; Jacobsen, N. E.; Polt, R. O-linked glycopeptides retain helicity in water. *J. Peptide Res.* **2001**, *58*, 180–189.
- (63) Lowery, J. J.; Raymond, T. J.; Giuvelis, D.; Bidlack, J. M.; Polt, R.; Bilsky, E. J. In vivo characterization of MMP-2200, a mixed  $\delta/\mu$  opioid agonist, in mice. *J. Pharm. Exp. Ther.* **2011**, *336*, 767–778.
- (64) Schiller, P. W. Bi- or multifunctional opioid peptide drugs. *Life Sci.* **2010**, *86*, 598–603.
- (65) Li, Y.; Lefever, M. R.; Muthu, D.; Bidlack, J. M.; Bilsky, E. J.; Polt, R. Opioid glycopeptide analgesics derived from endogenous enkephalins and endorphins. *Future Med. Chem.* **2012**, *4*, 205–226.
- (66) Lyu, P. C.; Sherman, J. C.; Chen, A.; Kallenbach, N. R. Alpha-helix stabilization by natural and unnatural amino acids with alkyl side chains. *Proc. Natl. Acad. Sci. U.S.A.* **1991**, *88*, 5317–5320.